Research Article | Vol. 27, No. 4 | 18 Feb 2019 | OPTICS EXPRESS 4077
Optics EXPRESS

Polariton-assisted splitting of broadband emission spectra of strongly coupled organic dye excitons in tunable optical microcavity

Dmitriy Dovzhenko,[1] Konstantin Mochalov,[2] Ivan Vaskan,[1,2,3] Irina Kryukova,[1] Yury Rakovich,[1,4,5,6] and Igor Nabiev[1,7,*]

[1]*National Research Nuclear University MEPhI (Moscow Engineering Physics Institute), Kashirskoe sh., 31, 115409 Moscow, Russia*
[2]*Shemyakin–Ovchinnikov Institute of Bioorganic Chemistry, Russian Academy of Sciences, Miklukho-Maklaya str., 16/10, 117997 Moscow, Russia*
[3]*Moscow Institute of Physics and Technology, 9 Institutskiy per., Dolgoprudny, 141701 Moscow, Russia*
[4]*Donostia International Physics Center, Paseo Manuel Lardizabal 4, 20018 Donostia-San Sebastián, Spain*
[5]*Centro de Física de Materiales (MPC, CSIC-UPV/EHU) and Donostia International Physics Center, Paseo Manuel de Lardizabal 5, 20018 Donostia-San Sebastian, Spain*
[6]*IKERBASQUE, Basque Foundation for Science, Maria Diaz de Haro 3, 48013 Bilbao, Spain*
[7] *Laboratoire de Recherche en Nanosciences, LRN-EA4682, Université de Reims Champagne-Ardenne, 51100 Reims, France*
[*]*igor.nabiev@univ-reims.fr*

Abstract: Resonance interaction between a localized electromagnetic field and excited states in molecules paves the way to control fundamental properties of a matter. In this study, we encapsulated organic molecules with relatively low unoriented dipole moments in the polymer matrix, placed them in tunable optical microcavity and realized, for the first time, controllable modification of the broad photoluminescence (PL) emission of these molecules in strong coupling regime at room temperature. Notably, while in most previous studies it was reported that the single mode dominates in the PL signal (radiation of the so-called branch of the lower polariton), here we report on the observation of two distinct PL peaks, evolution of which has been followed as the microcavity mode is detuned from the excitonic resonance. A significant Rabi splitting estimated from the modified PL spectra was as large as 225 meV. The developed approach can be used both in fundamental research of resonant light-mater coupling and its practical applications in sensing and development of coherent spontaneous emission sources using a combination of carefully designed microcavity with a wide variety of organic molecules.

1. Introduction

Light-matter coupling between dipole transitions in matter and the localized electromagnetic field is a central topic of cavity quantum electrodynamics research. It could lead to reversible coherent energy exchange between a single or an ensemble of emitters and a cavity mode [1–3]. This coupling imposes strict restrictions on system parameters and occurs only when the transition is in resonance with the electromagnetic mode. One of the main features of coupled systems is strong dependence of their properties on the interaction between the material and its local electromagnetic environment [4,5]. Thus, altering the environment by placing an emitter in a cavity can drastically affect the spectral properties in controlled manner [6–8]. In general, properties of a coupled system are governed by the competition between the rate of the coherent energy exchange (Rabi frequency) and the damping rates of the emitter and microcavity. Depending on the ratio between these rates, two coupling regimes can be distinguished: weak and strong coupling. Weak coupling regime takes place when damping

#355676 https://doi.org/10.1364/OE.27.004077
Journal © 2019 Received 18 Dec 2018; revised 25 Jan 2019; accepted 25 Jan 2019; published 4 Feb 2019

Optics EXPRESS

rates prevail over coupling rate [9]. In this regime, the spontaneous emission rate of the emitter is modified by altering the photon density of states, which is also known as Purcell effect [10]. This regime can be effectively used in photonics, biosensing and the development of many electro-optical devices [6,11,12]. Strong coupling regime is reached when energy exchange between the emitting dipole and the cavity mode is faster than their damping rates. Strong coupling leads to formation of the new eigenstates separated by the energy of the Rabi splitting that can be described in terms of hybridized light-matter bosonic quasiparticles called polaritons [13]. The fundamental properties of these new eigenstates originate from the quantum-mechanical superposition of the two original states. Thus, the implementation of strong coupling is of a special interest since in this regime the fundamental properties of coupled matter can be greatly altered. This effect can be used in a variety of applications, such as enhancement of Raman scattering [14], modifications of chemical reactivity [15], enhanced conductivity [16], nonradiative energy transfer [17–19] and fabrication of coherent spontaneous emission sources [20–22].

In general, Rabi splitting value ($\hbar\Omega_R$) for the ensemble of emitters could be estimated using the following equation [4]:

$$\hbar\Omega_R = 2\hbar g\sqrt{N} = 2F_{geom}d\sqrt{\frac{\hbar\omega N}{\varepsilon_0 V_m}}, \tag{1}$$

where g is the coupling strength, N is the number of coupled emitters, F_{geom} is the parameter depending on the spatial orientation of dipole moment and cavity mode distribution, d is the transition dipole moment, ω is the frequency of the cavity field, V_m is the mode volume, and ε_0 is the vacuum permittivity. Over the past decades, a strong coupling has been achieved by coupling emitter to selected optical modes of various resonators, which resulting in different values of Rabi splitting [3]. However, most of these systems consist of an emitter placed in a microcavity, which has fixed separation distance between two metal layers or distributed Bragg reflectors, which makes it laborious to study strong coupling effect for different samples since each sample requires unique set-up arrangement. This necessitates the development of a versatile experimental set-up based on open access microcavities with tunable parameters. In this regard, a tunable Fabry–Perot microcavity with opposite plane-convex mirrors is a great promising approach for the investigation of the strong coupling phenomenon [23,24]. Using this approach, a tunable microcavity cell (TMC) was recently developed in our group [25], which is equipped with interchangeable mirrors with different reflective indices, a piezo-positioner for adjustment of the resonator length, and a high-precision alignment system. Among the advantages of this design we would like to accentuate the availability of the optical mode for coupling to the electronic or vibronic states of freestanding molecules and nanoparticles, high-precision tunability of the resonance wavelength by precise control of cavity length using the piezoelectric actuator, and an open access to the TMC for effortless sample replacement. Furthermore, the variable distance between the mirrors provides an ability to directly measure the dispersion of polaritons and to demonstrate the avoided crossing between two (upper and lower) polariton branches in the spectra of hybrid states.

Since the achievement of the strong coupling regime requires a large coupling strength, which is proportional to the emitter dipole moment, it is necessary for the emitter to have a dipole moment as large as possible. The most effective way to significantly increase the dipole moment is to use the phenomenon of collective coupling [3]. In this case ensemble of coupled emitters act like one collective dipole due to the bosonic nature of polaritons [26]. Consequently, the coupling strength becomes proportional to the square root of the concentration of emitters in the ensemble [27]. In this regard, organic materials are a

Optics EXPRESS

particularly favorable choice, since they have large binding energies, can reach high densities and have large dipole moments through collective interaction.

Rhodamine 6G (R6G) is one of the most frequently used fluorescent molecule in many fundamental optical studies due to its high quantum yield of fluorescence (up to 100% [28]) in the visible range (500-600 nm) and significant absorption cross section [29–31]. Recently, the drastic change in emission properties of R6G has been demonstrated, such as the modulation of the emission spectrum, the fluorescence lifetime, and the fluorescence quantum yield, upon placing the molecules inside a metal microcavity with metal mirrors which were separated by a subwavelength spacer [32–34]. On the other hand, R6G has very broad absorption and emission bands, which makes it difficult to fulfill the requirements for strong coupling. It is noteworthy that some of the previous studies were performed using plasmonic modes for coupling with R6G transitions [29,30,35]. In these nanostructures, extremely small plasmonic mode volume leads to the considerable increase in the coupling strength. However, the coupling to the plasmonic modes has several fundamental disadvantages. The plasmonic mode cannot be changed or adjusted during the experiment and, therefore there is no possibility to make the coupling process tunable and reversible. Moreover, an ensemble of molecules assembled with plasmon structures is inaccessible for any other manipulations, and hence it becomes difficult to use such systems in practical applications. Besides, the close contact of organic molecules with the surface of the metal nanoparticles leads to a strong quenching of their emission due to the effective Förster resonance energy transfer.

Here we present results of the investigation of the emission properties of R6G molecules encapsulated in the Poly(methyl methacrylate) (PMMA) matrix, whose electronic transitions are coupled with electromagnetic modes of tunable optical microcavity at room temperature. The developed approach based on the use of an open-access microcavity for the controllable wide-range tuning of the coupling strength can be effectively used both in fundamental researches of resonant light-mater interaction and for practical applications of strong coupling phenomena in chemistry, biosensing, fabrication of optoelectronic devices and novel sources of coherent emission [16–22].

2. Materials and methods

2.1 Experimental setup

Scheme of the experimental setup consisting of the TMC and the light excitation/collection system, is shown on Fig. 1. The design and implementation of the TMC has been described elsewhere [25]. More specifically, TMC is a tunable unstable λ/2 Fabry–Perot microcavity consisting of plane and convex mirrors. This configuration satisfies the plane-parallelism condition, at least at one point of the curved mirror, and also minimizes the mode volume. Fine-adjustment of the microcavity length is provided by the Z-piezopositioner in the range up to 10 μm with a step of several nm. The moving console used for the upper interchangeable convex mirror holding is equipped with the XY precision positioner for the alignment of the plane-parallelism point and the sample. A sample was deposited directly on the bottom flat mirror, which consists of standard (18x18 mm) glass coverslips with Al films of different thicknesses on their upper side. The coverslips with a sample were glued to the interchangeable holders, which, in turn, were placed on Z-piezo-positioner of the TMC. The intracavity space was filled with Cargille Type DF (Cargille Labs) immersion oil. The TMC was placed on the homemade inverted confocal microspectrometer that included an Ntegra-base (NT-MDT) with a 100X/0.80 MPLAPON objective (Olympus) mounted on a Z-piezo-positioner, an XY scanning piezo-stage, and a confocal unit.

The light excitation/collection system consisted of a 488-nm Ar + laser (LGN-519M, Plazma Ltd.) with the power of 0.1 mW, an Andor Shamrock 750 monochromator equipped with an Andor DU971P-BV CCD (Andor Technology Ltd) and two 488-nm ultrasteep long-pass edge filters (RazorEdge, Semrock). To align the “area of interest” on the sample with the field of view of the confocal microspectrometer, the TMC can be adjusted in transverse plain

Optics EXPRESS

using the Ntegra-base XY-screws. A white LED (MCWHF2, Thorlabs) with a homemade optical condenser was used for broadband upper illumination of TMC.

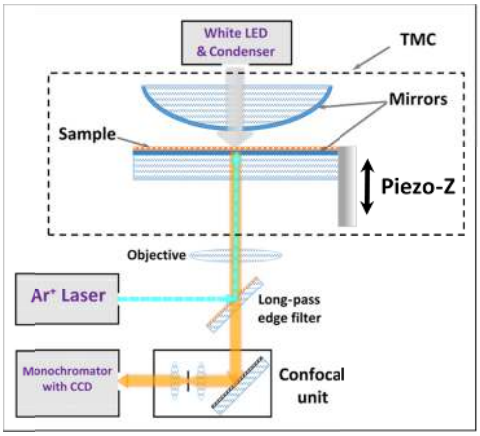

Fig. 1. Scheme of the experimental setup.An atomic force microscopy (AFM) imaging was carried out using of the unique setup "System for probe-optical 3D correlative microscopy" of the Institute of Bioorganic Chemistry of the Russian Academy of Sciences (IBCh RAS) (http://ckp-rf.ru/usu/486825/) [36,37]. Equipment was provided by the IBCh core facility (CKP IBCh, supported by Russian Ministry of Education and Science, grant RFMEFI62117X0018). High resolution of images has been achieved using silicon noncontact AFM-cantilevers (NSG01, Tipsnano OU).

2.2 Preparation and characterization of R6G-PMMA films

Poly(methyl methacrylate) (PMMA) thin films containing R6G were obtained using spin-coating method. First, a mixture of 10 µl of R6G in methanol and 1 mL of toluene solution of PMMA with intermediate chain length of 120k in concentration of 2 mg/mL and 25 mg/mL, respectively, were prepared. Then, 100 µL of R6G in PMMA was dropped on a substrate, namely, a pre-cleaned metal mirror covered with SiO_2 protective layer. At the next step, the substrate was rotated for 30 s at an angular velocity of 1000 rpm to ensure the evaporation of toluene. The AFM profiling technique was used to estimate the average thickness of the R6G-PMMA film. The measuring procedure is based on scratching a sample with a sharp blade followed by an AFM-imaging of the scratch area. AFM images were acquired in the semi-contact topography mode, and the size of the scanning area was in the all cases 25x25 µm (512x512 points) with the scanning rate of 0.8 Hz. It is noteworthy that the scratched substrate consists not only of the PMMA film but also has underneath the metal mirror. As a result, AFM profiling yields the total thickness of whole multilayer structure. Thus, it was first necessary to estimate the thickness of the metal films on bare mirrors. The values of ca 35 nm and ca 45 nm were obtained for the 67% reflection mirrors and the 87% reflection mirrors, respectively. The AFM-image of cross-section of the scratch in PMMA film deposited on the 87% reflection mirror is shown in Fig. 2(a). It can be seen that the total thickness of the 87% mirror and PMMA film was about 150 nm. Taking into account the average thickness of the metal coating for this mirror, the thickness of the R6G-PMMA film was estimated to be ca 105 nm.

Figure 2(b) shows the fluorescence spectrum of the R6G-PMMA film measured with the integration time of 3s. The uniformity of the distribution of R6G molecules in the PMMA matrix and hence through the whole area of a sample was monitored using the confocal fluorescence microspectroscopy. For the confocal fluorescent imaging, the fluorescence signal was integrated in the spectral range of 540–560 nm under the same excitation condition. The scan area was 50 × 50 µm (200 × 200 pixels), while the integration time was 0.1 s/point. The mean deviation of the fluorescence intensity over the whole scanning area did

Optics EXPRESS

not exceed 10%, which indicates a fairly uniform distribution of the dye. Transition dipole moment of R6G for main absorption peak was estimated to be about 1.74 D in [38].

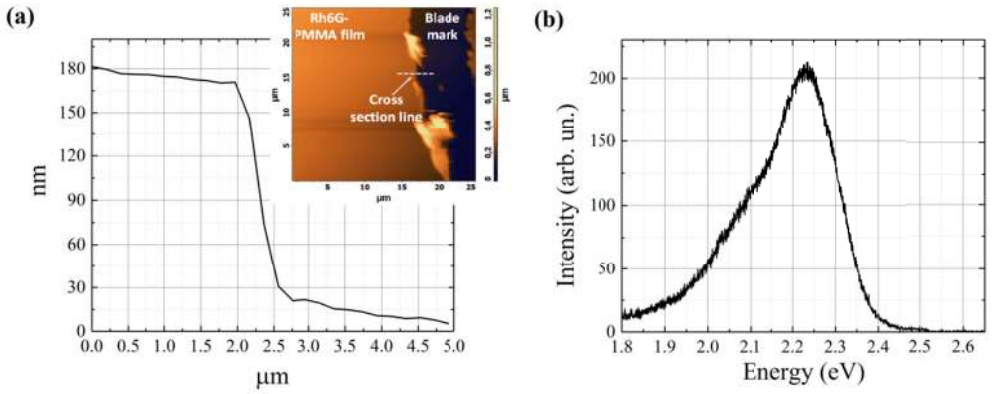

Fig. 2. (a) AFM-image (inset) and the cross-section of the scratch-in-PMMA area on the 87% reflection mirror. (b) Fluorescence spectrum of the R6G-PMMA film on metal mirror substrate.

2.3 Measurements of transmission and fluorescence spectra

The step-by-step TMC landing algorithm was described in detail elsewhere [25]. After the landing procedure was completed, all movements in Z-direction were performed exclusively with the Z piezo-positioner of the lower plane mirror. The distance between the two mirrors was monitored in real time from the analysis of the transmission spectra, which were recorded using white LED emission in the CCD continuous mode with 1s integration time.

For a given refractive index of the intracavity medium (immersion oil and the PMMA matrix), the estimated from the transmission spectra parameters – the free spectral range (distance between the resonance peaks) and the resonance quality-factor (Q-factor) - were directly related to the distance between the mirrors. It is important to point out that before measuring the spectra, the relative position of the mirrors was adjusted in manual close-loop mode until their complete halt. After this final adjustment of the mutual position of the mirrors, the transmission spectra were measured with an increased integration time of 3s. The fluorescence spectra were obtained at the same conditions as in p.2.2. The white LED was switched off and laser excitation was used instead.

3. Results and discussion

Above, we described the principal advantages of our TMC over conventional optical cavities consisting of two plane metal mirrors. Curved surface of one of the mirrors leads to much lower mode volumes and hence to increased coupling strength. Using optical measurements of transmission of empty cavity and comparing the results with the mathematical modelling, we have shown [39], that it is possible to achieve the mode volume two orders of magnitude lower, and the coupling strength more than an order of magnitude higher with respect to conventional optical cavities. These results have shown the possibility to fulfill strong coupling conditions for materials with lower dipole moments, wider absorption and luminescence spectra and to use lower concentrations than, for example, in ensembles of J-aggregates of cyanine dye. In this paper we used R6G in order to demonstrate the advantages of developed TMC in the case of a coupling of a broad electronic transitions in organic molecules to the modes of optical resonator. Previous study of the strong coupling phenomenon in ensembles of R6G molecules where carried out mainly using plasmonic nanoparticles [29,30,35] because of their much smaller mode volumes (around 10^{-5} in $\left(\frac{\lambda}{n}\right)^3$

Optics EXPRESS

units) in contrast to the value of 10^5 in the case of conventional optical resonators [3]. However, the use of the developed TMC with small mode volume allows not only to achieve the strong coupling regime in the optical microcavity, but also to make it in a tunable manner. Recently we have shown [39] that the mode volume of developed TMC could be as small as 73 in $\left(\frac{\lambda}{n}\right)^3$ units. Moreover, it can be tuned in a wide range, up to 10^5, with the corresponding tunability of the spectral position of transmission peaks and their Q-factor. As a result, it is possible to tune not only the energy of the coupled states, but also the coupling strength, as well as to investigate the properties of the same system in weakly or strongly coupled regimes in comparison to the properties of the uncoupled states of the exactly the same system. In order to eliminate the possibility of coupling of electronic transitions of R6G simultaneously with more than one longitudinal mode of the microcavity, the free spectral range of microcavity modes must be sufficiently wide. This means that there is an upper limit for the separation between mirrors. On the other hand, one of goals of this work was to maximize this separation in order to demonstrate the effect of the lateral confinement on the mode volumes and, consequently, show the potential for further development of TMC. Promisingly, even a distance of a few microns between the mirrors opens up the possibility of fabricating microfluidic channel on the surface of bottom mirror and achieving strong coupling regime in a dynamic flow of molecules. Furthermore, the damping rate of the optical modes should be significantly lower than that of R6G molecule. Otherwise it would be difficult to achieve the coupling rate high enough to overcome the damping rate of the whole system and make the coherent energy exchange dominant. To ensure that these conditions are met, we carried out all experiments with a mirror separation of about 2 micrometers and mirror reflection coefficients of 67% and 87%.

Another important feature of the developed setup is that at relatively low concentrations of R6G molecules in PMMA films, the number of photons from the white LED used for transmission measurements greatly overcomes the number of generated excitons, and most of the transmitted light passes the cavity uncoupled. As a result, the effect of coupling in transmission spectra cannot be observed. In contrast, in the case of fluorescence, the number of emitted photons fundamentally cannot exceed the number of excited excitons, and the requirement for a collective coupling observation can be fulfilled.

Figure 3 shows the normalized fluorescence spectrum measured from a cavity containing a R6G-PMMA film, as well as the transmission spectrum and fluorescence spectrum of R6G-PMMA film on a mirror. In this experiment, the distance between the mirrors was about 1830 nm, and the reflectivity of the mirrors was about 67%. The resulting Q-factor of the eigenmode was 140 and the free spectral range (FSR) was 0.22 eV.

Optics EXPRESS

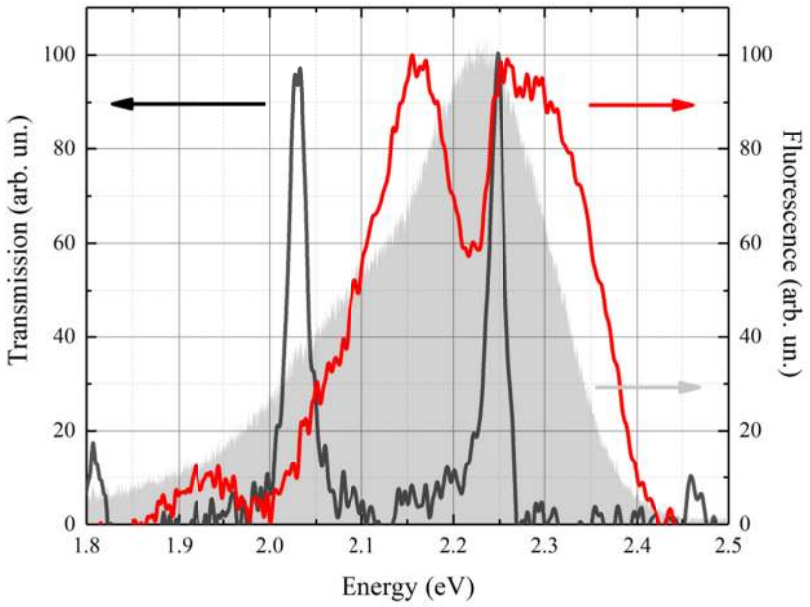

Fig. 3. Fluorescence spectrum (red curve) of R6G-PMMA film in a tunable microcavity in comparison to the fluorescence spectrum of the same film on the substrate (grey area) outside the microcavity and corresponding transmission spectrum of the microcavity (black curve).

The uncoupled emission of an ensemble of R6G molecules originates from both monomers and dimers of dye molecules contained in PMMA films. The monomers absorb at 2.35 eV and have an emission maximum at about 2.25 eV, while dimers, despite having two maxima in the absorption spectrum (at 2.48 and 2.26 eV), emit only from a lower energy state at 2.07 eV [40].

In general, aggregates of more than two R6G molecules and of excimers can also make a contribution to the emission spectra. However, this additional contribution is negligibly small, and monomer emission prevails in the fluorescence spectrum (Fig. 3). Thus, it is predominantly the monomeric electronic transitions that are involved in the formation of coupled states with the optical modes of the microcavity.

Figure 3 also demonstrates drastic modification of the lineshape of the fluorescence band of the R6G-PMMA film in TMC. The pronounced double-peak structure is observed now in the emission spectrum with the corresponding peak energies of 2.16 and 2.27 eV. It is important to note that the dip in the fluorescence spectrum between two maxima exactly coincides with the spectral position of the emission maximum of an ensemble of unbound R6G molecules, and is also shifted relative to the maxima in the transmission spectra of the cavity. Generally, in the case of a strong coupling of electronic transitions of all R6G molecules with photon modes, emission should not be observed at cavity eigenmode energies due to formation of hybrid energy states spectrally shifted from the microcavity eigenmodes. However, in the spectrum shown in Fig. 3, fluorescence is observed at the spectral position of the higher-energy eigenmode of the cavity. It can be explained by the contribution of emission from non-hybridized states, which could be additionally enhanced at the energies of the eigenmodes of the microcavity. Besides, the overall broad fluorescence spectrum of the R6G-PMMA film in a TMC may also be affected by the presence of uncoupled states and R6G aggregates, the fluorescence of which, weak in the case of uncoupled system, can also be enhanced by interaction with the microcavity modes. Nevertheless, the splitting energy in the fluorescence spectrum (about 110 meV) is quite large for the system of optical resonators

integrated with quantum emitters, but, strictly speaking, do not exceeds the broadening of the original emission spectrum of R6G film. Indeed, the full width at half maximum of the fluorescence spectrum of R6G monomers is estimated to be about 160 meV [30]. In order to achieve the maximum coupling strength and demonstrate the evolution of the energies of the two polaritonic branches, experiments were carried out in which the mirror separation was varied with a step of 30 nm while recording the emission spectra. In that way, the distance between the mirrors was changed from 1790 nm to 1970 nm, causing a corresponding variation of the eigenmode energies from 2.1 to 2.3 eV, which covers the entire area of maximum emission of the R6G film. The resulting fluorescence spectra are shown in Fig. 4.

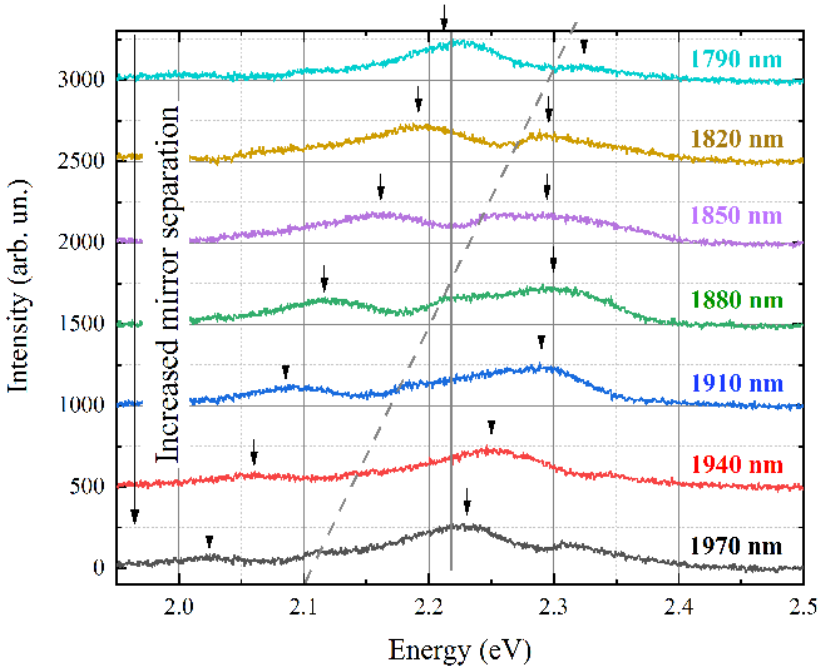

Fig. 4. Fluorescence spectra (color curves) of the R6G-PMMA film in a tunable microcavity with different distances between low (67%) reflecting mirrors. The spectra are vertically shifted for better presentation. From the upper spectra to the bottom one, the distance between the mirrors increased from 1790 nm to 1970 nm. Black arrows mark the maxima of the emission of the cavity polaritons. The corresponding spectral shift of the transmission maxima is marked with a dashed grey line. The solid grey line indicates the emission maximum of the R6G film without the microcavity.

The upper and lower spectra correspond to the maximum detuning of the maxima of cavity transmission from the maximum of the R6G fluorescence spectrum measured without a microcavity. The presented data clearly demonstrate the anti-crossing behavior of polaritonic branches. In all measured spectra, the most pronounced emission was observed in the spectral region of two separate peaks, which correspond to two hybridized modes. The only exception is one weak emission peak, which coincides in energy with the position of the transmission maximum of an empty microcavity, and is due to the contribution of a small number of unbound dye molecules. Similar mechanism of weak coupling but with the higher energy cavity mode leaded to the formation of additional peaks with the energy about 2.32 eV for black and red curves.

Optics EXPRESS

In the anti-crossing regime, the value of Rabi splitting, and, therefore, the coupling strength, can be deducted from the spectrum measured at zero detuning, when the resonator mode energy coincides with the energy of the emission maximum of R6G (about 2.22 eV). For these conditions, the Rabi splitting was estimated to be 184 meV. This value exceeds the emission bandwidth of the R6G film measured without a microcavity, and, thus strong coupling criteria are met.

It is important to note that while observation of Rabi splitting in extinction and reflection spectra of the hybrid systems combining organic dyes and confined electromagnetic field have been reported in a number of publications [3,29,30], investigation of hybrid states in fluorescence spectra is usually more complicated. Most often, only emission from the lower polaritonic branch is observed experimentally, in contrast to the case of extinction experiments, when both upper and lower polaritonic branches can be clearly detected. This peculiarity can be explained by the presence of uncoupled states in the ensemble of molecules, which leads to the prevailing fast recombination (of the order of 50 fs) from the upper hybrid state towards these uncoupled states [41]. It should be noted that the uncoupled states could also have delocalized character in case of discrete electromagnetic field spectrum [42]. However, in our experiments, a pronounced emission from both the upper and the lower polaritonic states was observed for all detunings. We speculate that it becomes possible because of the relatively low number of uncoupled states within the cavity mode volume, which leads to the suppression of recombination from the upper polaritonic branch to the uncoupled states.

Another interesting effect, observed in our experiments, is a rather unusual splitting behavior upon changing the detuning. After passing the point of zero detuning, the spectral position of high-energy emission peak abruptly shifts to the lower energies and gradually approaches the energy of the emission maximum the R6G film at 2.2 eV (Fig. 4, blue, red and gray curves). This behavior can be explained by taking into account the multi-component nature of the emission of an R6G film containing monomers, dimers and, very likely, various aggregates of dye molecules. Tuning the cavity photon energy leads to a drastic change in the probability of coupling of cavity eigenmodes with electronic transitions of different constituents of the R6G film. Electronic transitions in monomers, dimers and aggregates of R6G molecules have different dipole moments, which leads to different coupling strength between the respective transitions and microcavity eigenmodes. Similar dispersion has been demonstrated previously in coupled systems with broadband emitters [29,43].

The experiments, the results of which are shown in Fig. 4, were carried out using TMC mirrors with a relatively low reflectivity (67%), which imposed a limit on the Q-factor of the microcavity, and, in effect, on the coupling strength. A further increase in coupling strength was achieved by replacing the mirrors with those that have a higher reflectivity of about 87%.

In this case, a slight decrease in the distance between the mirrors along with an increase in reflectivity led to the increased Q-factor up to 187 and FSR of 0.29 eV. In line with the procedure used in previous experiment, the separation between the mirrors was gradually varied from 1424 to 1552 nm with a step of 26 nm. The corresponding eigenmode energies varied from 2.1 to 2.3 eV covering the area of the maximum in the emission spectrum of the R6G. The resulted fluorescence spectra are shown in Fig. 5.

Optics EXPRESS

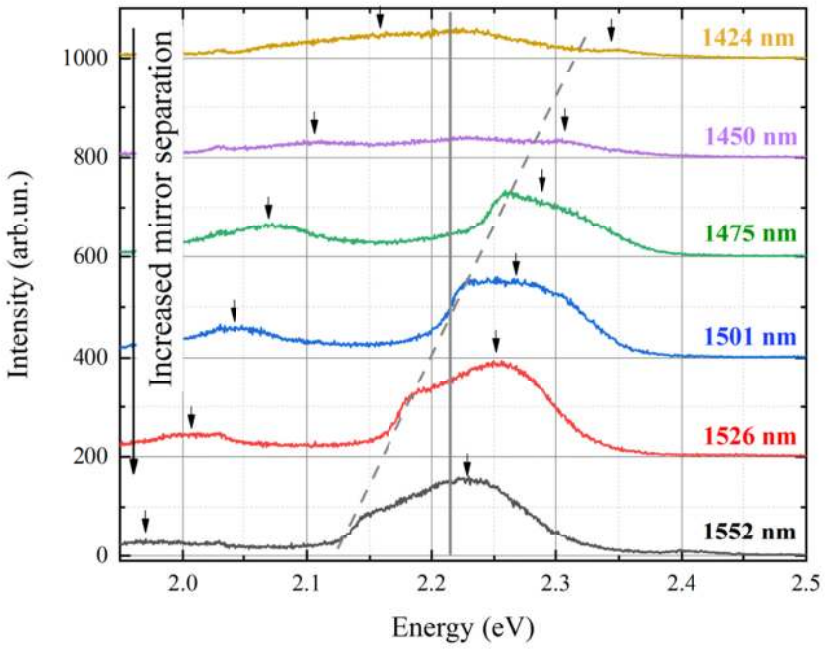

Fig. 5. Fluorescence spectra (color curves) of the R6G-PMMA film in a tunable microcavity with different distances between high (87%) reflecting mirrors. The spectra are vertically shifted for clarity. From the upper to the bottom one, the distance between the mirrors increased from 1424 nm to 1552 nm. Black arrows indicate the maxima of the emission of the cavity polaritons. The corresponding spectral shift of the transmission maxima is marked with dashed grey line. The solid grey line indicates the emission maximum of the R6G film without the microcavity.

As in the previous case, the upper and lower spectra correspond to the maximum detuning of cavity transmission peaks from the maximum in the fluorescence spectrum of the R6G measured without a microcavity. A clear anti-crossing behavior can be seen in Fig. 5, as well as an increase in the Rabi splitting energy, which correlate with the changes in the optical properties of the electromagnetic modes of the cavity. The Rabi splitting at zero detuning reached 225 meV, which is a rather large value for such system [3]. It is noteworthy that the emission detected at the energy of the cavity eigenmode has become relatively larger than in the previous case of a microcavity with lower reflectance of the mirrors. This can be explained with the assumption that some of R6G molecules embedded in a PMMA film are subjected to the effect of a weak coupling and a corresponding enhancement of emission. Such an enhancement is proportional to the square root of the Q-factor divided by the mode volume. The increased Q-factor of a microcavity with mirrors of increased reflectivity leads to the increase in the emission enhancement at the microcavity eigenmode energy.

4. Conclusions

We have demonstrated that the R6G emission can be controllably modified using light-matter interaction between the electronic transition of dye and the electromagnetic modes of a tunable open access optical microcavity, despite the relatively low value of the dipole moment and the broad emission band of the ensemble of the R6G molecules. For the first time both the upper and the lower polariton branches have been observed in the fluorescence

Optics EXPRESS

spectra in such a system. In the emission spectra of the R6G films placed in a tunable microcavity, a strong dependence of the polariton state energy on the distance between the mirrors of the microcavity, as well as clear anti-crossing behavior of two branches were demonstrated. By changing the cavity parameters, the polariton energy varied from 1.98 to 2.35 eV while experimenting with one sample. A large Rabi splitting energy of up to 225 meV was reached, which, we believe, is not the upper limit of this parameter. The achieved value of the Rabi splitting energy is bigger than the emission bandwidth of the R6G measured without a cavity, which fully satisfies the condition for a strong coupling regime. It is expected that significant enlargement can further be made by increasing the concentration R6G molecules. The demonstration of polariton emission from both the higher and the lower energy states in a tunable open access optical microcavity with a few micron distances between mirrors opens up great prospects. First of all, it is promising opportunity to use thick films placed in a microcavity, which can significantly increase the range of materials in which electronic transitions are strongly coupled to the cavity photons. The second valuable prospect is the feasibility to fabricate the versatile flow cell for a dynamic strong coupling of the transitions of molecules in a microfluidic channel. Such a system can be used for dynamic control of chemical reactions or highly effective bio- and chemical sensing in a flow cell. In addition, R6G is a widely used dye for lasing applications and with its electronic transitions being strongly coupled it can be used to create novel sources of exciton-polariton coherent spontaneous emission, as well as exciton-polariton lasers with a tunable emission wavelength.

Funding

Ministry of Education and Science of the Russian Federation (14.Y26.31.0011); Ministerio de Economiá y Competitividad (Fis 2016.80174-P, PLASMOQUANTA).

References

1. H. J. Kimble, “Strong interactions of single atoms and photons in cavity QED,” Phys. Scr. **T76**(1), 127–137 (1998).
2. J. McKeever, A. Boca, A. D. Boozer, J. R. Buck, and H. J. Kimble, “Experimental realization of a one-atom laser in the regime of strong coupling,” Nature **425**(6955), 268–271 (2003).
3. D. S. Dovzhenko, S. V. Ryabchuk, Y. P. Rakovich, and I. R. Nabiev, “Light-matter interaction in the strong coupling regime: configurations, conditions, and applications,” Nanoscale **10**(8), 3589–3605 (2018).
4. P. Törmä and W. L. Barnes, “Strong coupling between surface plasmon polaritons and emitters: a review,” Rep. Prog. Phys. **78**(1), 013901 (2015).
5. G. Khitrova, H. M. Gibbs, M. Kira, S. W. Koch, and A. Scherer, “Vacuum Rabi splitting in semiconductors,” Nat. Phys. **2**(2), 81–90 (2006).
6. S. Noda, M. Fujita, and T. Asano, “Spontaneous-emission control by photonic crystals and nanocavities,” Nat. Photonics **1**(8), 449–458 (2007).
7. B. Lee, J. Park, G. H. Han, H. S. Ee, C. H. Naylor, W. Liu, A. T. C. Johnson, and R. Agarwal, “Fano resonance and spectrally modified photoluminescence enhancement in monolayer MoS2 integrated with plasmonic nanoantenna array,” Nano Lett. **15**(5), 3646–3653 (2015).
8. D. S. Dovzhenko, E. V. Osipov, I. L. Martynov, P. A. Linkov, and A. A. Chistyakov, “Enhancement of spontaneous emission from CdSe/CdS/ZnS quantum dots at the edge of the photonic band gap in a porous silicon Bragg mirror,” Phys. Procedia **73**, 126–130 (2015).
9. V. A. Krivenkov, S. A. Goncharov, I. Nabiev, and Y. P. Rakovich, “Induced transparency in plasmon–exciton nanostructures for sensing applications,” Laser Photonics Rev., 1800176 (2018).
10. E. M. Purcell, “Spontaneous transition probabilities in radio-frequency spectroscopy,” Phys. Rev. **69**, 681 (1946).
11. M. Pelton, “Modified spontaneous emission in nanophotonic structures,” Nat. Photonics **9**(7), 427–435 (2015).
12. X. W. Yuan, L. Shi, Q. Wang, C. Q. Chen, X. H. Liu, L. X. Sun, B. Zhang, J. Zi, and W. Lu, “Spontaneous emission modulation of colloidal quantum dots via efficient coupling with hybrid plasmonic photonic crystal,” Opt. Express **22**(19), 23473–23479 (2014).
13. C. Weisbuch, M. Nishioka, A. Ishikawa, and Y. Arakawa, “Observation of the coupled exciton-photon mode splitting in a semiconductor quantum microcavity,” Phys. Rev. Lett. **69**(23), 3314–3317 (1992).
14. A. Shalabney, J. George, H. Hiura, J. A. Hutchison, C. Genet, P. Hellwig, and T. W. Ebbesen, “Enhanced Raman scattering from vibro-polariton hybrid states,” Angew. Chem. Int. Ed. Engl. **54**(27), 7971–7975 (2015).
15. A. Thomas, J. George, A. Shalabney, M. Dryzhakov, S. J. Varma, J. Moran, T. Chervy, X. Zhong, E. Devaux, C. Genet, J. A. Hutchison, and T. W. Ebbesen, “Ground-state chemical reactivity under vibrational coupling to the vacuum electromagnetic field,” Angew. Chem. Int. Ed. Engl. **55**(38), 11462–11466 (2016).

Optics EXPRESS

16. E. Orgiu, J. George, J. A. Hutchison, E. Devaux, J. F. Dayen, B. Doudin, F. Stellacci, C. Genet, J. Schachenmayer, C. Genes, G. Pupillo, P. Samorì, and T. W. Ebbesen, "Conductivity in organic semiconductors hybridized with the vacuum field," Nat. Mater. **14**(11), 1123–1129 (2015).
17. G. G. Rozenman, K. Akulov, A. Golombek, and T. Schwartz, "Long-range transport of organic exciton-polaritons revealed by ultrafast microscopy," ACS Photonics **5**(1), 105–110 (2017).
18. X. Zhong, T. Chervy, L. Zhang, A. Thomas, J. George, C. Genet, J. A. Hutchison, and T. W. Ebbesen, "Energy transfer between spatially separated entangled molecules," Angew. Chem. Int. Ed. Engl. **56**(31), 9034–9038 (2017).
19. X. Zhong, T. Chervy, S. Wang, J. George, A. Thomas, J. A. Hutchison, E. Devaux, C. Genet, and T. W. Ebbesen, "Non-radiative energy transfer mediated by hybrid light-matter states," Angew. Chem. **128**(21), 6310–6314 (2016).
20. H. Deng, G. Weihs, D. Snoke, J. Bloch, and Y. Yamamoto, "Polariton lasing vs. photon lasing in a semiconductor microcavity," Proc. Natl. Acad. Sci. U.S.A. **100**(26), 15318–15323 (2003).
21. T. Guillet, M. Mexis, J. Levrat, G. Rossbach, C. Brimont, T. Bretagnon, B. Gil, R. Butté, N. Grandjean, L. Orosz, F. Réveret, J. Leymarie, J. Zúñiga-Pérez, M. Leroux, F. Semond, and S. Bouchoule, "Polariton lasing in a hybrid bulk ZnO microcavity," Appl. Phys. Lett. **99**(16), 161104 (2011).
22. M. Ramezani, A. Halpin, A. I. Fernández-Domínguez, J. Feist, S. R. K. Rodriguez, F. J. Garcia-Vidal, and J. G. Rivas, "Plasmon-exciton-polariton lasing," Optica **4**(1), 31–37 (2017).
23. A. Konrad, A. M. Kern, M. Brecht, and A. J. Meixner, "Strong and coherent coupling of a plasmonic nanoparticle to a subwavelength Fabry–Pérot resonator," Nano Lett. **15**(7), 4423–4428 (2015).
24. A. Chizhik, F. Schleifenbaum, R. Gutbrod, A. Chizhik, D. Khoptyar, A. J. Meixner, and J. Enderlein, "Tuning the fluorescence emission spectra of a single molecule with a variable optical subwavelength metal microcavity," Phys. Rev. Lett. **102**(7), 073002 (2009).
25. K. E. Mochalov, I. S. Vaskan, D. S. Dovzhenko, Y. P. Rakovich, and I. Nabiev, "A versatile tunable microcavity for investigation of light-matter interaction," Rev. Sci. Instrum. **89**(5), 053105 (2018).
26. B. M. Garraway, "The Dicke model in quantum optics: Dicke model revisited," Philos Trans A Math Phys Eng Sci **369**(1939), 1137–1155 (2011).
27. G. S. Agarwal, "Vacuum-Field Rabi Splittings in Microwave Absorption by Rydberg Atoms in a Cavity," Phys. Rev. Lett. **53**(18), 1732–1734 (1984).
28. C. Würth, M. G. González, R. Niessner, U. Panne, C. Haisch, and U. R. Genger, "Determination of the absolute fluorescence quantum yield of rhodamine 6G with optical and photoacoustic methods--providing the basis for fluorescence quantum yield standards," Talanta **90**, 30–37 (2012).
29. T. K. Hakala, J. J. Toppari, A. Kuzyk, M. Pettersson, H. Tikkanen, H. Kunttu, and P. Törmä, "Vacuum Rabi splitting and strong-coupling dynamics for surface-plasmon polaritons and rhodamine 6G molecules," Phys. Rev. Lett. **103**(5), 053602 (2009).
30. N. I. Cade, T. Ritman-Meer, and D. Richards, "Strong coupling of localized plasmons and molecular excitons in nanostructured silver films," Phys. Rev. B Condens. Matter Mater. Phys. **79**(24), 241404 (2009).
31. P. Vasa, W. Wang, R. Pomraenke, M. Lammers, M. Maiuri, C. Manzoni, G. Cerullo, and C. Lienau, "Real-time observation of ultrafast Rabi oscillations between excitons and plasmons in metal nanostructures with J-aggregates," Nat. Photonics **7**(2), 128–132 (2013).
32. B. Zhen, S. L. Chua, J. Lee, A. W. Rodriguez, X. Liang, S. G. Johnson, J. D. Joannopoulos, M. Soljačić, and O. Shapira, "Enabling enhanced emission and low-threshold lasing of organic molecules using special Fano resonances of macroscopic photonic crystals," Proc. Natl. Acad. Sci. U.S.A. **110**(34), 13711–13716 (2013).
33. R. Sasai, T. Itoh, W. Ohmori, H. Itoh, and M. Kusunoki, "Preparation and characterization of rhodamine 6G/alkyltrimethylammonium/laponite hybrid solid materials with higher emission quantum yield," J. Phys. Chem. C **113**(1), 415–421 (2008).
34. V. Martínez Martínez, F. López Arbeloa, J. Bañuelos Prieto, and I. López Arbeloa, "Characterization of rhodamine 6G aggregates intercalated in solid thin films of laponite clay. 2 Fluorescence spectroscopy," J. Phys. Chem. B **109**(15), 7443–7450 (2005).
35. S. R. K. Rodriguez and J. G. Rivas, "Surface lattice resonances strongly coupled to Rhodamine 6G excitons: tuning the plasmon-exciton-polariton mass and composition," Opt. Express **21**(22), 27411–27421 (2013).
36. K. E. Mochalov, A. A. Chistyakov, D. O. Solovyeva, A. V. Mezin, V. A. Oleinikov, I. S. Vaskan, M. Molinari, I. I. Agapov, I. Nabiev, and A. E. Efimov, "An instrumental approach to combining confocal microspectroscopy and 3D scanning probe nanotomography," Ultramicroscopy **182**, 118–123 (2017).
37. A. E. Efimov, I. I. Agapov, O. I. Agapova, V. A. Oleinikov, A. V. Mezin, M. Molinari, I. Nabiev, and K. E. Mochalov, "A novel design of a scanning probe microscope integrated with an ultramicrotome for serial block-face nanotomography," Rev. Sci. Instrum. **88**(2), 023701 (2017).
38. G. Zengin, T. Gschneidtner, R. Verre, L. Shao, T. J. Antosiewicz, K. Moth-Poulsen, M. Käll, and T. Shegai, "Evaluating conditions for strong coupling between nanoparticle plasmons and organic dyes using scattering and absorption spectroscopy," J. Phys. Chem. C **120**(37), 20588–20596 (2016).
39. D. S. Dovzhenko, I. S. Vaskan, K. E. Mochalov, Y. P. Rakovich, and I. Nabiev, "Spectral and spatial characteristics of the electromagnetic field modes in the tunable optical microcavity cell for the investigation of the "light-matter" hybrid state," JETP Lett. **109**(1), 12–18 (2019).
40. M. Chapman, M. Mullen, E. Novoa-Ortega, M. Alhasani, J. F. Elman, and W. B. Euler, "Structural evolution of ultrathin films of rhodamine 6G on glass," J. Phys. Chem. C **120**(15), 8289–8297 (2016).

Optics EXPRESS

41. V. Agranovich, M. Litinskaia, and D. Lidzey, "Cavity polaritons in microcavities containing disordered organic semiconductors," Phys. Rev. B Condens. Matter Mater. Phys. **67**(8), 085311 (2003).
42. C. Gonzalez-Ballestero, J. Feist, E. Gonzalo Badía, E. Moreno, and F. J. Garcia-Vidal, "Uncoupled dark states can inherit polaritonic properties," Phys. Rev. Lett. **117**(15), 156402 (2016).
43. S. Betzold, S. Herbst, A. A. P. Trichet, J. M. Smith, F. Würthner, S. Höfling, and C. P. Dietrich, "Tunable light–matter hybridization in open organic microcavities," ACS Photonics **5**(1), 90–94 (2018).